



# Modeling Co toxicity effects on *Acidithiobacillus ferrooxidans* for environmentally sustainable recycling of Lithium-Ion batteries

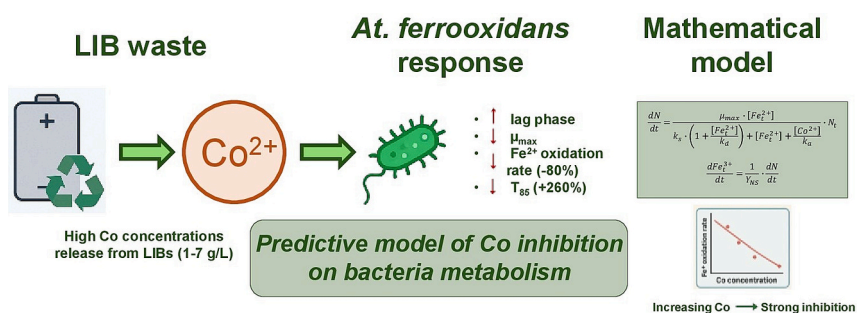
Alessia Amato, Alessandro Becci\*, Francesca Beolchini

Department of Life and Environmental Sciences, Università Politecnica delle Marche, Via Brecce Bianche, Ancona 60131, Italy

## HIGHLIGHTS

- Co showed higher toxicity than Cu, Cd, Ni, Zn, As, except Cr.
- A mathematical model was built to explore Co toxicity in detail.
- Co above 5 g/L cuts Fe oxidation rate by more than 80%

## GRAPHICAL ABSTRACT



## ARTICLE INFO

**Keywords:**  
*At. ferrooxidans*  
 Toxicity  
 Mathematical modelling  
 Sensitivity analysis  
 Biotechnology

## ABSTRACT

The rapid expansion of lithium-ion battery (LIB) production, driven by the rise of electric vehicles and renewable energy storage, has led to growing concerns about end-of-life management and critical material recovery. In this context, biotechnological processes represent an environmentally sustainable alternative to conventional recycling methods such as pyrometallurgy and hydrometallurgy, offering reduced impacts on both ecosystems and human health. However, the performance of bioleaching systems depends heavily on microbial tolerance to toxic metals released from LIBs.

This study focuses on assessing the toxicological effects of Co, a key strategic metal in LIBs, on *Acidithiobacillus ferrooxidans*, a model organism for bioleaching applications. Experimental findings reveal that Co exhibits greater toxicity than Cu, Cd, Ni, Zn, and As, but is less toxic than Cr. Co concentrations exceeding 5 g/L result in a 260% increase in Fe<sup>2+</sup> oxidation time and an 80% reduction in the Fe oxidation rate. Additionally, elevated Co levels significantly prolong the exponential growth phase, indicating metabolic stress.

A predictive mathematical model was developed and validated to describe bacterial growth and Fe<sup>2+</sup> oxidation under varying Co concentrations, achieving a determination coefficient (R<sup>2</sup>) above 0.95. This model serves as a practical tool for optimizing process parameters in the bio-recycling of LIBs, enabling more efficient and scalable engineering applications.

These findings contribute to the advancement of greener technologies for critical raw material recovery and support the integration of bio-based methods into circular economy strategies for battery waste management.

\* Corresponding author.

E-mail address: [a.becci@univpm.it](mailto:a.becci@univpm.it) (A. Becci).

<https://doi.org/10.1016/j.biortech.2026.134312>

Received 1 September 2025; Received in revised form 9 February 2026; Accepted 27 February 2026

Available online 28 February 2026

0960-8524/© 2026 The Authors. Published by Elsevier Ltd. This is an open access article under the CC BY license (<http://creativecommons.org/licenses/by/4.0/>).

## 1. Introduction

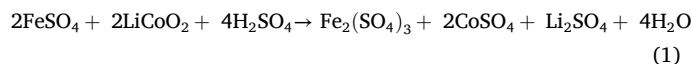
The growing awareness of environmental and climate-related challenges has led to a global commitment toward a more sustainable future, emphasizing the urgent transition from a fossil fuel-based economy to renewable energy systems (European Commission, 2021). Given the intermittency of renewable sources, energy storage technologies have become essential components of this transition, playing a crucial role in both the energy and transport sectors, together responsible for approximately 70% of global greenhouse gas emissions (Agency, 2022).

Among various energy storage devices, LIBs have gained prominence due to their high energy density (120 W\*hrs/kg), long lifespan (500–10000 cycles), wide operating temperature range (−20 to 60 °C), and absence of toxic heavy metals (such as Cd or Pb) (Al-Thyabat et al., 2013). These characteristics make LIBs particularly suitable for applications in portable electronics and electric vehicles (Fergus, 2010). Over the past two decades, LIB production has grown exponentially, alongside increasing research and development efforts (Zeng et al., 2014). However, this surge in production is also leading to a significant increase in spent LIBs, with projections estimating the generation of over 460,000 tons of waste batteries in 2025, and nearly 2 million tons by 2040 (Chen et al., 2019; Zhao et al., 2019).

LIBs contain critical raw materials such as Li and Co, whose limited availability and geographically concentrated reserves raise concerns about supply security and long-term sustainability (Chen et al., 2019; Pazik et al., 2016; Salazar and McNutt, 2021). In recognition of this, both Li and Co have been included in the European Union's list of Critical Raw Materials (European Commission, 2023). The recycling of LIBs has therefore emerged as a key strategy to reduce environmental impact and mitigate resource scarcity by recovering valuable secondary raw materials (Ferronato and Torretta, 2019; Mossali et al., 2020; Nnorom and Osibanjo, 2009).

Current recycling technologies include pyrometallurgical and hydrometallurgical processes, both of which are widely studied and applied at industrial scale (Lv et al., 2018). However, these methods often involve high energy consumption or the generation of hazardous waste (Cerrillo-Gonzalez et al., 2020; Lv et al., 2018; Mossali et al., 2020). In response, biohydrometallurgy, an emerging field that utilizes microorganisms to produce leaching agents, offers a potentially more sustainable alternative (Roy et al., 2021c, 2021b, 2021a). This biological approach can significantly reduce the environmental footprint associated with conventional acid-based leaching processes while achieving high recovery rates of metals such as Li and Co. As such, biohydrometallurgy represents a promising avenue in the development of a circular economy for LIBs, aligning technological innovation with environmental sustainability. One of the most studied microorganisms for LIBs leaching is *At. ferrooxidans* (Mishra et al., 2008; Naseri et al., 2019a; Roy et al., 2021c, 2021b, 2021a; Sethurajan and Gaydardzhiev, 2021; Zhang et al., 2018). The main limitation of biotechnological processes is the low solid concentration (between 1 and 10%), which results from the toxicity of metals on bacterial metabolism (Becci et al., 2021; Liu et al., 2020; Wu et al., 2020; Zhang et al., 2023). While acidophilic bacteria exhibit high tolerance toward certain metals (such as Ni, Cu, and Zn (Roy et al., 2021a)), the toxicity of Co, one of the metals with the highest concentrations in LIBs (~ 19% w/w), has been poorly investigated (Wu et al., 2020). According to the literature, the average metal concentrations in LIBs are approximately 5% for Li, 14% for Mn, 8% for Ni, 6% for Al, 1% for Fe, and 5% for Cu (Bahaloo-Horeh et al., 2018; Boxall et al., 2018; Heydarian et al., 2018; Horeh et al., 2016; Kim et al., 2024; Panda et al., 2024; Roy et al., 2021c; Wang et al., 2022; Xin et al., 2016).

Co, which is present in LIBs in the form of an oxide, is extracted in biotechnological processes with acidophilic bacteria (e.g. *At. ferrooxidans*) through the following redox reactions (Eqs. 1–2) (Heydarian et al., 2018; Liu et al., 2020; Roy et al., 2021b; Zhang et al., 2023):



Co is an essential micronutrient for acidophilic bacteria at  $\mu\text{M}$  concentrations, as it plays a key role in the biosynthesis of vitamin B<sub>12</sub> (Nies and Grass, 2009). However, at elevated concentrations, the redox-active nature of Co promotes the generation of reactive oxygen species (ROS), leading to oxidative stress and cellular damage (Fantino et al., 2010; Wu et al., 2020). The presence of Co has been shown to impair the cellular radical scavenging system, resulting in the accumulation of ROS, primarily superoxide anions (O<sub>2</sub><sup>-</sup>) (Liu et al., 2014; Wu et al., 2020). Superoxide dismutase (SOD), a key antioxidant enzyme responsible for the dismutation of O<sub>2</sub><sup>-</sup>, is inhibited by Co exposure, further exacerbating oxidative stress within the cells (Kurhaluk and Tkachenko, 2016; Wu et al., 2020).

Given the high Co concentrations typically found in LIBs and its documented toxicity toward acidophilic bacterial communities, this study aims to elucidate the effects of Co on both *At. ferrooxidans* growth dynamics and metabolic activity.

## 2. Materials and methods

### 2.1. Toxicity test

*At. ferrooxidans* (DSMZ 14882 t) was provided as pure culture by Deutsche Sammlung von Mikroorganismen und Zellkulturen GmbH (DSMZ) of the Leibniz Institute. Bacteria were cultured in DSMZ 882 medium, containing 0.132 g/L (NH<sub>4</sub>)<sub>2</sub>SO<sub>4</sub>, 0.053 g/L MgCl<sub>2</sub>·6H<sub>2</sub>O, 0.027 g/L KH<sub>2</sub>PO<sub>4</sub> and 0.147 g/L CaCl<sub>2</sub>·2H<sub>2</sub>O, as well as electron donor FeSO<sub>4</sub>·7H<sub>2</sub>O at a concentration of 20 g/L and H<sub>2</sub>SO<sub>4</sub> for a pH value of 1.5. The toxicity of Co towards *At. ferrooxidans* was tested by inoculating the bacteria (10% v/v) in a modified growth medium containing different concentrations of soluble Co<sup>2+</sup> (1, 3, 5, 7 g/L). Co was dissolved in the medium as CoSO<sub>4</sub>·7H<sub>2</sub>O. The maximum concentration of 7 g/L was chosen by simulating a complete leaching of LIBs at a concentration of 4% (w/v), based on the average Co concentration reported in the literature. Previous studies have shown that the Co leaching yields started to decrease at this LIB concentration in biotechnological processes (Heydarian et al., 2018; Kim et al., 2024; Naseri et al., 2019a,b; Panda et al., 2024; Roy et al., 2021b; Wang et al., 2022). Bacteria were inoculated in the different modified mediums at their exponential growth phase. The cultures were then kept shaken (120 rpm) for 96 hrs (4 days) at room temperature, and pH was re-established to a pH value of 1.5 once a day to avoid the Fe<sup>3+</sup> precipitation (Amato et al., 2020; Becci et al., 2020). All the experiments were carried out in double. Despite this, the reproducibility between replicates was high (SD < 10%), supporting the reliability of the results.

### 2.2. Analytical methods

The quantitative analysis of the Fe concentration and its speciation was carried out through a spectrophotometric determination. Samples were withdrawn periodically (15, 19, 24, 39, 43, 48, 63, 72 and 96 h) for the Fe<sup>3+</sup> determination, it was useful to study the bacteria activity and metabolism during the time. The Fe<sup>3+</sup> present in the samples was coloured with potassium thiocyanate (KSCN) (ratio sample:KSCN of 1:1 (v/v)) and spectrophotometrically detected at 480 nm (Jasco model 7850) (Becci et al., 2021; Welcher and Hahn, 1964).

The estimation of the total bacterial number (N°/mL) was carried out through the direct count technique (Becci et al., 2021; Danovaro et al., 2002; Zimmermann, 1977). Samples were taken after 15, 24, 48, 72 and 96 h to evaluate bacterial growth over time. The analysed samples were firstly fixed in formalin, then diluted to obtain a final count of

approximately 10–20 bacteria per optical field. Two replicates at the final dilution were prepared for each initial sample. Each replicate was firstly incubated with Acridine Orange (final concentration of 0,025% w/v) and then pressured-filtered on a sterile polycarbonate membrane (0.22  $\mu\text{m}$ ). The membranes were then positioned on sterile glass microscope slides.

Slides were analysed using an epifluorescence microscope at  $\lambda = 450\text{--}490\text{ nm}$  and 1000X magnification. As described in the protocol, the bacterial number of each replicate was obtained as an average of the bacterial counts obtained from 20 different and random optical fields. The  $N^\circ/\text{mL}$  for each replicate was then calculated through the following equation (Eq. (3)):

$$\frac{N^\circ}{\text{mL}} = \frac{N \cdot CO \cdot d}{\text{mL}} \quad (3)$$

where  $N$  is the mean bacteria number per optical section,  $CO$  is the maximum optical section number (12,868),  $d$  is the sample dilution, and  $\text{mL}$  is the withdraw solution (0.5 mL).

### 2.3. Mathematical model to predict Co toxicity on *At. ferrooxidans*

The experimental results were used to fit the model and to determine the best parameters to describe the bacteria number and  $\text{Fe}^{3+}$  temporal profile. The parameters were estimated by the nonlinear least square procedure by a modification of the Levenberg – Marquardt algorithm (Marquardt, 1963; Moré, 1978). In the model used, the bacterial growth rate (Eq. (4)) and the  $\text{Fe}^{3+}$  production rate (Eq. (5)) were assumed to follow the model described by Harvey and Crundwell (1997) (Eq. (6)) (Harvey and Crundwell, 1997). This model is a modification of the Monod equation (Monod, 1949), that relates the bacterial growth to the use of limiting nutrient  $\text{Fe}^{2+}$ , the inhibition of the product ( $\text{Fe}^{3+}$ ) factor and the toxicity factor of the heavy metal.

$$\frac{dN_t}{dt} = \mu \cdot N_t \quad (4)$$

$$\frac{d\text{Fe}_t^{3+}}{dt} = \frac{1}{Y_{NS}} \cdot \frac{dN_t}{dt} \quad (5)$$

$$\mu = \frac{\mu_{max} \cdot [\text{Fe}_t^{2+}]}{k_s \cdot \left(1 + \frac{[\text{Fe}_t^{2+}]}{k_d}\right) + [\text{Fe}_t^{2+}] + \frac{[\text{Co}]}{k_a}} \quad (6)$$

Where  $N$  is the bacterial number ( $N^\circ/\text{mL}$ ),  $\text{Fe}^{2+}$  and  $\text{Fe}^{3+}$  are the concentrations of the Fe species (g/L),  $Co$  is the concentration of Co (g/L),  $\mu_{max}$  (1/h) is the maximum specific growth rate,  $k_s$  (g/L) is the substrate saturation constant,  $k_d$  (g/L) is the inhibition parameter due to the  $\text{Fe}^{3+}$  effects,  $k_a$  (g/L) is the toxicity index due to Co and  $Y_{NS}$  ( $N^\circ/\text{gFe}^{2+}$ ) is the bacteria yield on substrate ( $\text{Fe}^{2+}$ ).

The five parameters ( $Y_{NS}$ ,  $\mu_{max}$ ,  $k_s$ ,  $k_p$  and  $k_a$ ) were estimated by fitting the equations (Eq. 4–6) to the experimental data obtained in the bacterial growth and activity analysis. The derived equations were solved using the Levenberg–Marquardt algorithm (Kenneth Levenberg, 1944). In the Levenberg–Marquardt algorithm the parameters of the model are chosen so that the residual deviation between observed and estimated data is minimized (Kenneth Levenberg, 1944).

### 2.4. Sensitivity analysis

A sensitivity analysis was performed on the parameters estimated by the mathematical model to investigate their correlations and assess how they influence the model's fit to the experimental data. The 95% confidence intervals for the parameters were derived from the variance–covariance matrix, computed using the minpack.lm package. The corresponding correlation matrix was obtained directly from this variance–covariance matrix. To explore parameter uncertainty, 1,000

random parameter sets were generated using a normal distribution centred on the best-fit values, with standard deviations equal to the estimated standard errors (via the rnorm function). Negative parameter values were excluded from the simulations. The 95% confidence regions for all variables were then visualized. A global sensitivity analysis of the parameters was also performed using the Wasserstein–Bures index to identify which parameters had the greatest impact on the final outcome (using the gsaot package). All calculations and parameter estimations were carried out using R software (version 2025.05.1 + 513).

## 3. Results and discussion

The study was conducted through a series of experiments involving varying concentrations of Co, alongside a control culture. From the experimental data, two key parameters were derived to aid in the interpretation of results:

- $T_{85}$ : the time required to oxidize 85% of the  $\text{Fe}^{2+}$  substrate (h), and
- BP (Bacterial Production): the amount of  $\text{Fe}^{2+}$  oxidized per bacterium per h (mg  $\text{Fe}_{\text{oxid}}^{2+}/\text{bacterium}\cdot\text{h}$ ).

The values of these parameters for each ion concentration and culture conditions are summarized in Table 1.

It is evident that the presence of Co reduced the oxidative capacity of the studied bacterial species (*At. ferrooxidans*), and furthermore, cell growth was inhibited with increasing metal concentrations in the medium (Fig. 1). The  $\text{Fe}^{2+}$  oxidation profile in the presence of different Co concentrations are shown in Fig. 1b. Increasing metal concentrations led to a progressive extension of the oxidation time: approximately 24 h in the control (this result is consistent with findings reported in previous studies (Becci et al., 2021; Cabrera et al., 2005a; Pourhossein and Mousavi, 2018; Tavakoli et al., 2021)), with about a 60% increase in the time required to oxidize 85% of the substrate at 1 g/L Co, and up to a 260% increase at the highest Co concentration tested (Co 7 g/L) (Table 1). A concentration of 5 g/L of Co produced effects comparable to those reported in previous toxicity assays conducted with 10 g/L of Cu and Cd, and 30 g/L of Ni, all resulting in approximately 70 h for the oxidation of 85% of  $\text{Fe}^{2+}$ . Conversely, a concentration of 3 g/L of Co resulted in  $T_{85}$  (around 50 h) values comparable to those observed for Zn and Cr at the concentration of 30 and 0.4 g/L, respectively (Cabrera et al., 2005a). Similar trends were also observed for BP. These findings suggest that Co, even at significantly lower concentrations, exhibits a toxicological impact similar to that of Cu, Cd, Zn and Ni at higher concentrations, thereby indicating a relatively higher acute toxicity, except for Cr. The presence of  $\text{Cr}^{3+}$  inhibits the ferro-cytochrome *c* reductase located in the cell membrane, thereby decreasing the ability of *At. ferrooxidans* to oxidize  $\text{Fe}^{2+}$ . In contrast, Co does not inhibit the enzymes involved in  $\text{Fe}^{2+}$  transport but leads to an increased production of ROS, resulting in oxidative stress (Wu et al., 2020). This delay is mirrored by a reduction in cell growth, as shown in the examples presented in Fig. 1a, where high Co concentrations result in a pronounced lag phase. However, *At. ferrooxidans* exhibits greater resistance to Co compared to other bacteria. At concentrations around 7 g/L ( $\sim 120\text{ mM}$ ), the bacterium is still able to grow, although its growth rate and metabolism are reduced. In contrast, other bacteria such as *L. ferriphilum*, *E. coli*, and *G. sulfurreducens* can tolerate only lower concentrations, up to a

**Table 1**  
 $T_{85}$  and BP for a pure culture of *At. ferrooxidans* in the presence of Co.

$\text{Co}^{2+}$ concentration (g/L)	$T_{85}$ (h)	BP (mg $\text{Fe}_{\text{oxid}}^{2+}/\text{bacterium}\cdot\text{h}$ )
0	24 $\pm$ 1	0.190 $\pm$ 0.002
1	39 $\pm$ 5	0.13 $\pm$ 0.03
3	54 $\pm$ 9	0.10 $\pm$ 0.03
5	72 $\pm$ 9	0.07 $\pm$ 0.02
7	87 $\pm$ 7	0.05 $\pm$ 0.01

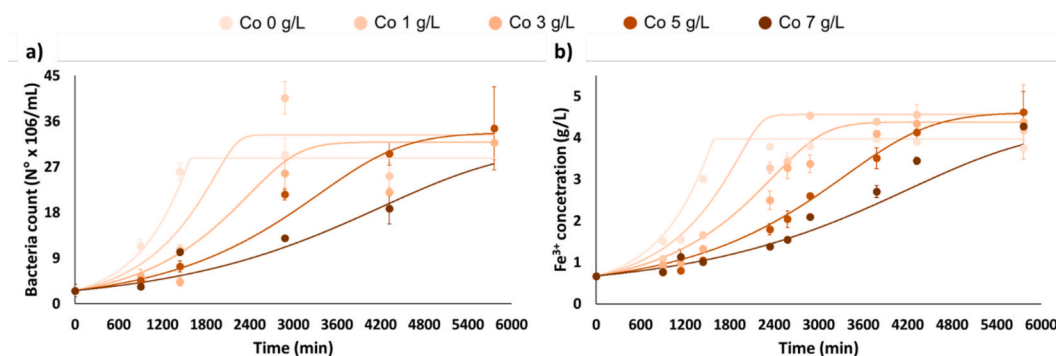


**Fig. 1.** Evolution of bacterial growth (a) and the Fe<sup>3+</sup> concentration trend (b) in the presence of several concentrations of Co (from 0 to 7 g/L). The points and the lines are the experimental and the differential equations (Eq.s 4–6) results, respectively. The bacteria growth is carried out for 4 days at room temperature and with 4 g/L of Fe<sup>2+</sup>. Reported are mean values and standard errors calculated from two independent replicates.

maximum of 5–10 mM Co (Dulay et al., 2020; Fantino et al., 2010; Nies and Grass, 2009; Wu et al., 2020).

Bacterial counts (N°/mL) and Fe<sup>3+</sup> concentrations (g/L) obtained from these experiments were used to calibrate the differential equations (Eq.s 4 and 5). Model parameters were estimated by minimizing the sum of squared errors between experimental data and model predictions (Harvey and Crundwell, 1997). The parameters  $k_s$ ,  $k_d$ ,  $k_a$ ,  $Y_{NS}$  in the differential equations were held constant across all tested conditions, as previous studies have shown that these parameters are not significantly influenced by metal-induced toxicity on bacterial growth (Harvey and Crundwell, 1997). In contrast, the maximum specific growth rate ( $\mu_{max}$ ) exhibited a marked decrease with increasing inhibitor concentrations in the medium (Becci et al., 2021; Cabrera et al., 2005b, 2005a; Harvey and Crundwell, 1997).

The numerical solutions, in which all parameters were held constant except for  $\mu_{max}$ , closely aligned with the experimental data, yielding coefficients of determination ( $R^2$ ) greater than 0.95 (Fig. 1). This high level of agreement indicates that the model reliably captures the dynamics of bacterial growth and Fe metabolism.

The parameters that describe the bacteria growth rate ( $\mu_{max}$ ), the substrate saturation constant ( $k_s$ ), the inhibition parameter due to the Fe<sup>3+</sup> effects ( $k_d$ ) and the bacteria yield on the substrate ( $Y_{NS}$ ) were in the range reported in the literature, between 0.06 and 0.25 1/h, 0.024 and 2.02 g/L, 0.06 and 0.315 g/L and  $0.25 - 5.9 \times 10^7$  N°/g Fe<sup>2+</sup>, respectively (Boon et al., 1999; Cabrera et al., 2005b; Chavarie et al., 2009; Kumar and Gandhi, 1990; Molchanov et al., 2007; Nemati et al., 1998; Rashidi et al., 2012). On the other hand, the  $k_a$  value ( $3 \pm 1$  g/L) estimated in this study is higher than the value previously reported for assessing As toxicity ( $2.0 \pm 0.2$  g/L), suggesting that Co exerts a slightly greater inhibitory effect on the metabolic activity of *At. ferrooxidans* compared to As (Harvey and Crundwell, 1997). The global sensitivity analysis showed that the parameters exerting the greatest influence on the results for bacterial growth and Fe<sup>2+</sup> oxidation are  $Y_{NS}$  (bacteria yield on substrate) and  $k_a$  (the Co-induced toxicity index). Other parameters that strongly affect the final outcomes are the  $\mu_{max}$  values determined for each individual Co concentration, whereas the remaining parameters ( $k_s$  and  $k_d$ ) exhibited a minor influence on the results.

The estimated parameters and the resulting differential equations were used to analyse the oxidation rate of Fe<sup>2+</sup> driven by bacterial metabolism under varying Co concentrations. In the control test (Co 0), the maximum Fe<sup>2+</sup> oxidation rate was observed approximately 25 h after the onset of bacterial growth, reaching a value of about 4.6 mg Fe<sup>2+</sup>/L·h (Fig. 2). The results show a progressive decline in the Fe<sup>2+</sup> oxidation rate with increasing Co concentrations, culminating in a minimum rate of approximately 0.8 mg Fe<sup>2+</sup>/L·h at the highest Co level tested (Co 7 g/L), corresponding to a reduction of roughly 82%. This minimum rate was reached around 70 h after the beginning of bacterial growth (Fig. 2). These findings are consistent with previous observations

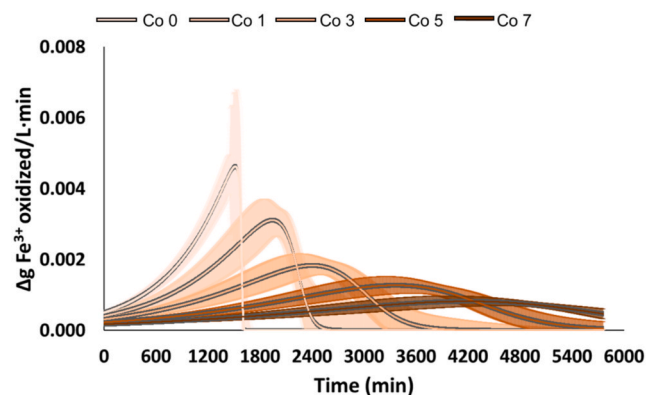


**Fig. 2.** Fe<sup>2+</sup> oxidation rate by bacteria metabolism at different Co concentrations (0, 1, 3, 5, 7 represent Co conc. in g/L). The bacteria growth is carried out for 4 days at room temperature and with 4 g/L of Fe<sup>2+</sup>. The graph shows the mean values (lines, oxidation rate calculated using the model's best-fit parameters) and the corresponding standard deviations (shaded areas, oxidation rate computed using the 1,000 parameter sets estimated by the model).

and results obtained using  $T_{85}$  and BP parameters.

To validate and strengthen the reliability of the parameters estimated by the mathematical model, a statistical analysis was conducted to evaluate the correlations among them. The estimated values for the maximum specific growth rate ( $\mu_{max}$ ) showed a consistent decrease with increasing Co concentration. The correlation analysis revealed a strong relationship among most of the  $\mu_{max}$  values, with correlation coefficients exceeding  $\pm 0.65$ . However,  $\mu_{max}$  values at Co 0 exhibited no significant correlation with those at Co 5 and Co 7, as indicated by correlation coefficients close to 0.

To further support these observations, confidence ellipses between the  $\mu_{max}$  of the control condition (Co 0) and those obtained at different Co concentrations (Co 1, Co 3, Co 5, and Co 7 g/L) were also analysed, providing more detailed insights into the correlation patterns and associated standard errors (Fig. 3a). A significant correlation ( $r = 0.79$ ) was observed between  $k_s$  and  $k_d$  (Table 1). This relationship is clearly illustrated in Fig. 3b, where an increase in  $k_s$  corresponds to a proportional increase in  $k_d$ . In contrast,  $k_a$  did not show any relevant correlation with  $k_s$  or  $k_d$ . However,  $k_a$  exhibited a strong negative correlation with  $\mu_{max}$  across different Co concentrations. This correlation became more pronounced with increasing Co levels, ranging from  $-0.76$  to  $-0.91$ , indicating that higher Co concentrations led to a more marked decrease in  $\mu_{max}$ , thereby reflecting an increase in Co-induced toxicity.

Given the observed decrease in  $\mu_{max}$  with increasing Co concentrations, a correlation between these two parameters was investigated. A non-linear regression analysis was performed to fit the determined  $\mu_{max}$

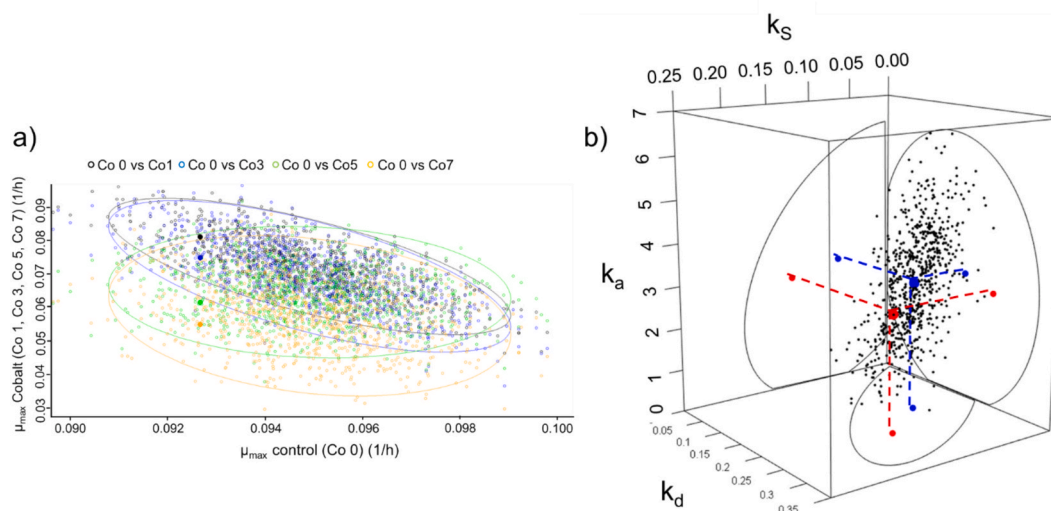


**Fig. 3.** Shown are the 95% confidence ellipses along with 1,000 randomly generated parameter values: (a) Distribution of values around the estimated  $\mu_{\max}$  at different Co concentrations; (b) Parameter space for constants  $k_s$ ,  $k_d$  and  $k_a$  as determined by the mathematical model, red points represent the best-fitting parameter sets, while blue points indicate the centres of the ellipses.

at different Co concentration by the mathematical model using the characteristic equation for non-competitive inhibition (Eq. (7)), describing the apparent maximum specific growth rate (Arsalan and Younus, 2018; Cabrera et al., 2005b).

$$\mu_{\max}^* = \frac{\mu_{\max} \cdot k_I}{[Co^{2+}] + k_I} \quad (7)$$

In this context,  $\mu_{\max}^*$  represents the maximum specific growth rate estimated for each experiment at different Co concentrations,  $k_I$  is the inhibition constant, and  $[Co^{2+}]$  denotes the Co concentration in the medium. An inhibition constant was calculated for each of the 1000 possible combinations of  $\mu_{\max}$  values obtained from the mathematical model and the sensitivity analysis at varying Co concentrations, yielding a mean  $k_I$  value of  $11 \pm 5$  (Fig. 4a). The  $k_I$  value obtained in this study supports the previous findings based on the  $T_{85}$  and BP parameters. Specifically, this value is lower than the inhibition constants reported for Cu, Cd, Zn, and Ni in earlier work (with a value of 20.92, 47.01, 131.52 and 89.23, respectively) (Cabrera et al., 2005b), confirming that Co is more toxic to *At. ferrooxidans* than these metals. However, Co appears to be less toxic than Cr, that reports a  $k_I$  value of 0.42 (Cabrera et al., 2005b, 2005a). The determined  $k_I$  value allowed for accurate estimation of  $\mu_{\max}$  at each Co concentration, with a coefficient of determination ( $R^2$ ) greater than 0.97 (Fig. 4b). Thanks to the determined  $k_I$  value, it will be possible to calculate  $\mu_{\max}$  at different Co concentrations and, by applying the previously developed and validated model equations, to study and predict the bacterial growth and metabolism. This will allow the model to be used for the design and optimization of the biotechnological

process for Co recovery from LIBs.

Finally, all possible scenarios resulting from the mathematical model and sensitivity analysis were evaluated, based on 1,000 parameter combinations. The resulting output distributions were analysed to identify the probability ranges corresponding to the various outcomes by combining all possible solutions. The results show that the full range of modelled outcomes effectively describes the experimental data in detail. In addition, the likelihood of the simulations converging to the same final outcome was estimated.

Regarding the 1,000 combinations of parameters in the control experiment (Co 0), 100% of the simulations predicted  $Fe^{2+}$  oxidation efficiencies greater than 95% within the first 24–26 h. For the parameter sets corresponding to Co concentrations of 1 and 3 g/L, over 97% of the simulations predicted  $Fe^{2+}$  oxidation by bacteria exceeding 95% within 96 h. For Co concentrations of 5 g/L, 85% of the simulations predicted  $Fe^{2+}$  oxidation above 90%, while the remaining 15% fell within an efficiency range of 70–90%. Finally, for Co concentrations of 7 g/L, only 20% of the simulations indicated  $Fe^{2+}$  oxidation above 90%, whereas the remaining 80% fell within the 50–90% range, with a higher probability (~20%) of achieving efficiencies between 85% and 90% (Fig. 5).

#### 4. Conclusions

This study demonstrated that Co is a toxic metal for the metabolism of *At. ferrooxidans*. The estimated parameters ( $T_{85}$ , BP,  $k_a$ , and  $k_I$ ) revealed that Co exhibits higher toxicity than Cu, Cd, Zn, Ni, and As, based on comparisons with values reported in previous studies on the

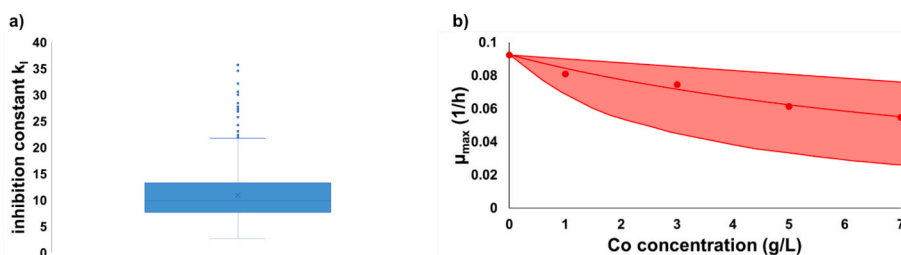


**Fig. 4.** (a) Boxplot of the 1000  $k_I$  values estimated using the non-competitive inhibition equation; (b) Range of estimated  $\mu_{\max}$  at different Co concentrations corresponding to different  $k_I$  values. Points represent the best-fit  $\mu_{\max}$  values obtained from the mathematical model (Eqs. (4)–(6)). The line shows the theoretical values calculated using the non-competitive inhibition equation with average parameter estimates, while the shaded area represents the range of the 1,000 theoretical values computed using the same equation.

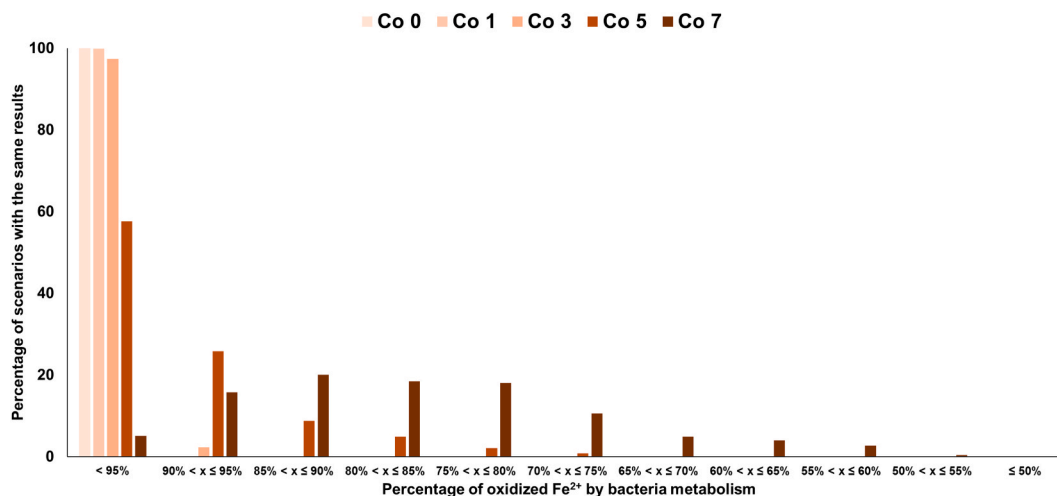


Fig. 5. Probability of achieving Fe<sup>2+</sup> oxidation efficiencies under different parameter combinations at varying Co concentrations.

same bacterial species. Cr was the only metal found to be more toxic than Co. At Co concentrations above 5 g/L, bacterial metabolism and growth were significantly inhibited. The Fe<sup>2+</sup> oxidation time increased by more than 260% compared to control conditions, while the Fe<sup>2+</sup> oxidation rate decreased by approximately 80%. Additionally, the presence of Co led to a prolonged lag phase in bacterial growth. These effects of Co on the slowdown of bacterial growth and metabolism would result in a considerable increase in the time required to complete a biotechnological process using *At. ferrooxidans* to treat end-of-life LIBs, leading to higher economic costs and reduced environmental sustainability of such an approach, thereby making biotechnologies less attractive for industrial-scale development.

Furthermore, the mathematical model developed in this study accurately simulated the temporal dynamics of both Fe<sup>2+</sup> oxidation and bacterial growth. This represents a valuable starting point and a useful model; however, it will need to be further developed to investigate the combined toxic effects of Co with other metals present in LIBs (e.g., Li, Ni, Mn, and Al). Therefore, this work should be regarded as an initial step toward studying the interactions among these metals and assessing whether they result in a greater or lesser inhibition of Fe oxidation. Furthermore, the ongoing replacement of Co with Ni in the production of new batteries, given the latter's lower toxicity, could further enhance the applicability of biotechnological approaches for end-of-life LIB treatment, promoting them as a more environmentally sustainable alternative.

#### CRedit authorship contribution statement

**Alessia Amato:** Writing – original draft, Visualization, Resources, Project administration, Methodology. **Alessandro Becci:** Writing – original draft, Visualization, Validation, Software, Methodology, Investigation, Formal analysis, Data curation, Conceptualization. **Francesca Beolchini:** Writing – original draft, Supervision, Resources, Project administration, Funding acquisition, Data curation, Conceptualization.

#### Declaration of competing interest

The authors declare that they have no known competing financial interests or personal relationships that could have appeared to influence the work reported in this paper.

#### Acknowledgements

This work was supported by the BRAVE project, funded under the

Italian Strategic Investment Fund (FIS-2023-03296). The authors are grateful to Maddalena Rugolo for his precious collaboration in the experimental work.

#### Appendix A. Supplementary data

Supplementary data to this article can be found online at <https://doi.org/10.1016/j.biortech.2026.134312>.

#### Data availability

Data will be made available on request.

#### References

- Agency, I.E., 2022. Global Energy Review : CO2 Emissions in 2021 Global emissions rebound sharply to highest ever level INTERNATIONAL ENERGY.
- Al-Thyabat, S., Nakamura, T., Shibata, E., Iizuka, A., 2013. Adaptation of minerals processing operations for lithium-ion (LiBs) and nickel metal hydride (NiMH) batteries recycling: critical review. *Miner. Eng.* 45, 4–17. <https://doi.org/10.1016/j.mineng.2012.12.005>.
- Amato, A., Becci, A., Beolchini, F., 2020. Sustainable recovery of Cu, Fe and Zn from end-of-life printed circuit boards. *Resour. Conserv. Recycl.* 158, 104792. <https://doi.org/10.1016/j.resconrec.2020.104792>.
- Arsalan, A., Younus, H., 2018. Enzymes and nanoparticles: Modulation of enzymatic activity via nanoparticles. *Int. J. Biol. Macromol.* 118, 1833–1847. <https://doi.org/10.1016/j.ijbiomac.2018.07.030>.
- Bahaloo-Horeh, N., Mousavi, S.M., Baniyadi, M., 2018. Use of adapted metal tolerant *Aspergillus niger* to enhance bioleaching efficiency of valuable metals from spent lithium-ion mobile phone batteries. *J. Clean. Prod.* 197, 1546–1557. <https://doi.org/10.1016/j.jclepro.2018.06.299>.
- Becci, A., Amato, A., Fonti, V., Karaj, D., Beolchini, F., 2020. An innovative biotechnology for metal recovery from printed circuit boards. *Resour. Conserv. Recycl.* 153. <https://doi.org/10.1016/j.resconrec.2019.104549>.
- Becci, A., Amato, A., Rodríguez-Maroto, J.M., Beolchini, F., 2021. Bioleaching of End-of-Life Printed Circuit Boards: Mathematical Modeling and Kinetic Analysis. *Ind. Eng. Chem. Res.* 60, 4261–4268. <https://doi.org/10.1021/acs.iecr.0c05566>.
- Boon, M., Ras, C., Heijnen, J.J., 1999. The ferrous iron oxidation kinetics of *Thiobacillus ferrooxidans* in batch cultures. *Appl. Microbiol. Biotechnol.* 51, 813–819. <https://doi.org/10.1007/s002530051467>.
- Boxall, N.J., Cheng, K.Y., Bruckard, W., Kaksonen, A.H., 2018. Application of indirect non-contact bioleaching for extracting metals from waste lithium-ion batteries. *J. Hazard. Mater.* 360, 504–511. <https://doi.org/10.1016/j.jhazmat.2018.08.024>.
- Cabrera, G., Gómez, J.M., Cantero, D., 2005a. Influence of heavy metals on growth and ferrous sulphate oxidation by *Acidithiobacillus ferrooxidans* in pure and mixed cultures. *Process Biochem.* 40, 2683–2687. <https://doi.org/10.1016/j.procbio.2004.12.005>.
- Cabrera, G., Gómez, J.M., Cantero, D., 2005b. Kinetic study of ferrous sulphate oxidation of *Acidithiobacillus ferrooxidans* in the presence of heavy metal ions. *Enzyme Microb. Technol.* 36, 301–306. <https://doi.org/10.1016/j.enzmictec.2004.09.008>.
- Cerrillo-Gonzalez, M., Villen-Guzman, M., Acedo-Bueno, L.F., Rodríguez-Maroto, J. M., Paz-García, J.M., 2020. Hydrometallurgical Extraction of Li and Co from LiCoO<sub>2</sub> Particles—Experimental and Modeling. *Appl. Sci.* 10, 6375. <https://doi.org/10.3390/app10186375>.

- Chavarie, C., Karamanev, D., Godard, F., Garnier, A., Chimique, D.D.G., Polytechnique, E., 2009. Comparison of the kinetics of ferrous iron oxidation by three different strains of *Thiobacillus ferrooxidans*. *Geomicrobiol. J.* 11, 37–41. <https://doi.org/10.1080/01490459309377932>.
- Chen, M., Ma, X., Chen, B., Arsenault, R., Karlson, P., Simon, N., Wang, Y., 2019. Recycling End-of-Life Electric Vehicle Lithium-Ion Batteries. *Joule* 3, 2622–2646. <https://doi.org/10.1016/j.joule.2019.01.014>.
- Danovaro, R., Manini, E., Dell'Anno, A., 2002. Higher Abundance of Bacteria than of Viruses in Deep Mediterranean Sediments. *Appl. Environ. Microbiol.* 68, 1468–1472. <https://doi.org/10.1128/AEM.68.3.1468-1472.2002>.
- Dulay, H., Tabares, M., Kashefi, K., Reguera, G., 2020. Cobalt Resistance via Detoxification and Mineralization in the Iron-reducing Bacterium *Geobacter sulfurreducens*. *Front. Microbiol.* 11, 1–17. <https://doi.org/10.3389/fmicb.2020.600463>.
- European Commission, 2023. Study on the critical Raw Materials for the EU 2023 Final Report. European Commission. <https://doi.org/10.2873/725585>.
- European Commission, 2021. In focus: Batteries – a key enabler of a low-carbon economy [WWW Document]. accessed 12.15.25. [https://commission.europa.eu/news-and-media/news/focus-batteries-key-enabler-low-carbon-economy-2021-03-15\\_en](https://commission.europa.eu/news-and-media/news/focus-batteries-key-enabler-low-carbon-economy-2021-03-15_en).
- Fantino, J.R., Py, B., Fontecave, M., Barras, F., 2010. A genetic analysis of the response of *Escherichia coli* to cobalt stress. *Environ. Microbiol.* 12, 2846–2857. <https://doi.org/10.1111/j.1462-2920.2010.02265.x>.
- Fergus, J.W., 2010. Recent developments in cathode materials for lithium ion batteries. *J. Power Sources* 195, 939–954. <https://doi.org/10.1016/j.jpowsour.2009.08.089>.
- Ferronato, N., Torretta, V., 2019. Waste Mismanagement in developing Countries: a Review of Global Issues. *Int. J. Environ. Res. Public Health* 16, 1060. <https://doi.org/10.3390/ijerph16061060>.
- Harvey, P.I., Crundwell, F.K., 1997. Growth of *Thiobacillus ferrooxidans*: a novel experimental design for batch growth and bacterial leaching studies. *Appl. Environ. Microbiol.* 63, 2586–2592. <https://doi.org/10.1128/aem.63.7.2586-2592.1997>.
- Heydari, A., Mousavi, S.M., Vakilchah, F., Baniasadi, M., 2018. Application of a mixed culture of adapted acidophilic bacteria in two-step bioleaching of spent lithium-ion laptop batteries. *J. Power Sources* 378, 19–30. <https://doi.org/10.1016/j.jpowsour.2017.12.009>.
- Horeh, N.B., Mousavi, S.M., Shojaosadati, S.A., 2016. Bioleaching of valuable metals from spent lithium-ion mobile phone batteries using *Aspergillus Niger*. *J. Power Sources* 320, 257–266. <https://doi.org/10.1016/j.jpowsour.2016.04.104>.
- Kenneth Levenberg, 1944 A Method for the solution of Certain Non-Linear Problems in Least Squares Q. *Appl. Math.* 2 1944 164 168 <https://doi.org/10.1066-0/S0033-569X-1944-10666-0>.
- Kim, J., Nwe, H.H., Yoon, C.S., 2024. Enhanced bioleaching of spent Li-ion batteries using a ferroxidans by application of external magnetic field. *J. Environ. Manage.* 367, 122012. <https://doi.org/10.1016/j.jenvman.2024.122012>.
- Kumar, S., Gandhi, K.S., 1990. Modelling of Fe<sup>2+</sup> oxidation by *Thiobacillus ferrooxidans*. *Appl. Microbiol. Biotechnol.* 33, 524–528. <https://doi.org/10.1007/BF00172545>.
- Kurhaluk, N., Tkachenko, H., 2016. Modulators of KATP channels in the prevention of oxidative stress and antioxidant capacity improvement in the rat heart with different resistance to hypoxia upon cobalt treatment. *J. Vet. Res.* 60, 195–206. <https://doi.org/10.1515/jvetres-2016-0029>.
- Liu, L., Xu, P., Zeng, G., Huang, D., Zhao, M., Lai, C., Chen, M., Li, N., Huang, C., Wang, C., Cheng, M., He, X., Lai, M., He, Y., 2014. Inherent antioxidant activity and high yield production of antioxidants in *Phanerochaete chrysosporium*. *Biochem. Eng. J.* 90, 245–254. <https://doi.org/10.1016/j.bej.2014.06.014>.
- Liu, X., Liu, H., Wu, W., Zhang, X., Gu, T., Zhu, M., Tan, W., 2020. Oxidative stress Induced by Metal Ions in Bioleaching of LiCoO<sub>2</sub> by an Acidophilic Microbial Consortium. *Front. Microbiol.* 10, 1–17. <https://doi.org/10.3389/fmicb.2019.03058>.
- Lv, W., Wang, Z., Cao, H., Sun, Y., Zhang, Y., Sun, Z., 2018. A critical Review and Analysis on the Recycling of Spent Lithium-Ion Batteries. *ACS Sustain. Chem. Eng.* 6, 1504–1521. <https://doi.org/10.1021/acsschemeng.7b03811>.
- Marquardt, D.W., 1963. An Algorithm for Least-Squares Estimation of Nonlinear Parameters. *J. Soc. Ind. Appl. Math.* 11, 431–441. <https://doi.org/10.1137/0111030>.
- Mishra, D., Kim, D.-J., Ralph, D.E., Ahn, J.-G., Rhee, Y.-H., 2008. Bioleaching of metals from spent lithium ion secondary batteries using *Acidithiobacillus ferrooxidans*. *Waste Manag.* 28, 333–338. <https://doi.org/10.1016/j.wasman.2007.01.010>.
- Molchanov, S., Gendel, Y., Ioslvich, I., Lahav, O., 2007. Improved experimental and computational methodology for determining the kinetic equation and the extant kinetic constants of Fe(II) oxidation by *Acidithiobacillus ferrooxidans*. *Appl. Environ. Microbiol.* 73, 1742–1752. <https://doi.org/10.1128/AEM.01521-06>.
- Monod, J., 1949. THE GROWTH OF BACTERIAL CULTURES. *Annu. Rev. Microbiol.* 3, 371–394. <https://doi.org/10.1146/annurev.mi.03.100149.002103>.
- Moré, J.J., 1978. The Levenberg-Marquardt algorithm: Implementation and Theory. In: *Analysis, N. (Ed.), Springer, Berlin, Heidelberg*, pp. 105–116.
- Mossali, E., Picone, N., Gentilini, L., Rodríguez, O., Pérez, J.M., Colledani, M., 2020. Lithium-ion batteries towards circular economy: a literature review of opportunities and issues of recycling treatments. *J. Environ. Manage.* 264, 110500. <https://doi.org/10.1016/j.jenvman.2020.110500>.
- Naseri, T., Bahaloo-Horeh, N., Mousavi, S.M., 2019a. Bacterial leaching as a green approach for typical metals recovery from end-of-life coin cells batteries. *J. Clean. Prod.* 220, 483–492. <https://doi.org/10.1016/j.jclepro.2019.02.177>.
- Naseri, T., Bahaloo-Horeh, N., Mousavi, S.M., 2019b. Environmentally friendly recovery of valuable metals from spent coin cells through two-step bioleaching using *Acidithiobacillus thiooxidans*. *J. Environ. Manage.* 235, 357–367. <https://doi.org/10.1016/j.jenvman.2019.01.086>.
- Nemati, M., Harrison, S.T.L., Hansford, G.S., Webb, C., 1998. Biological oxidation of ferrous sulphate by *Thiobacillus ferrooxidans*: a review on the kinetic aspects. *Biochem. Eng. J.* 1, 171–190. [https://doi.org/10.1016/S1369-703X\(98\)00006-0](https://doi.org/10.1016/S1369-703X(98)00006-0).
- Nies, D.H., Grass, G., 2009. Transition Metal Homeostasis. *EcoSal plus* 3. <https://doi.org/10.1128/ecosalplus.5.4.4.3>.
- Nnorom, I.C., Osibanjo, O., 2009. Heavy metal characterization of waste portable rechargeable batteries used in mobile phones. *Int. J. Environ. Sci. Technol.* 6, 641–650. <https://doi.org/10.1007/BF03326105>.
- Panda, S., Dembele, S., Mishra, S., Akcil, A., Agcasulu, I., Hazrati, E., Tuncuk, A., Malavasi, P., Gaydardzhiev, S., 2024. Small-scale and scale-up bioleaching of Li, Co, Ni and Mn from spent lithium-ion battery. *J. Chem. Technol. Biotechnol.* 99, 1069–1082. <https://doi.org/10.1002/jctb.7609>.
- Pazik, P.M., Chmielewski, T., Glass, H.J., Kowalczyk, P.B., 2016. World production and possible recovery of cobalt from the Kupferschiefer stratiform copper ore. *E3S Web Conf.* 8, 01063. <https://doi.org/10.1051/e3sconf/20160801063>.
- Pourhossein, F., Mousavi, S.M., 2018. Enhancement of copper, nickel, and gallium recovery from LED waste by adaptation of *Acidithiobacillus ferrooxidans*. *Waste Manag.* 79, 98–108. <https://doi.org/10.1016/j.wasman.2018.07.010>.
- Rashidi, A., Safdari, J., Roosta-azad, R., Zokaei-kadijani, S., 2012. Annals of Nuclear Energy Modeling of uranium bioleaching by *Acidithiobacillus ferrooxidans*. *Ann. Nucl. Energy* 43, 13–18. <https://doi.org/10.1016/j.anucene.2011.12.020>.
- Roy, J.J., Cao, B., Madhavi, S., 2021a. A review on the recycling of spent lithium-ion batteries (LIBs) by the bioleaching approach. *Chemosphere* 282, 130944. <https://doi.org/10.1016/j.chemosphere.2021.130944>.
- Roy, J.J., Madhavi, S., Cao, B., 2021b. Metal extraction from spent lithium-ion batteries (LIBs) at high pulp density by environmentally friendly bioleaching process. *J. Clean. Prod.* 280, 124242. <https://doi.org/10.1016/j.jclepro.2020.124242>.
- Roy, J.J., Srinivasan, M., Cao, B., 2021c. Bioleaching as an Eco-Friendly Approach for Metal Recovery from Spent NMC-Based Lithium-Ion Batteries at a High Pulp Density. *ACS Sustain. Chem. Eng.* 9, 3060–3069. <https://doi.org/10.1021/acsschemeng.0c06573>.
- Salazar, K., McNutt, M.K., 2021. Mineral Commodity Summaries. <https://doi.org/10.3133/MCS2021>.
- Sethurajan, M., Gaydardzhiev, S., 2021. Bioprocessing of spent lithium ion batteries for critical metals recovery – a review. *Resour. Conserv. Recycl.* 165, 105225. <https://doi.org/10.1016/j.resconrec.2020.105225>.
- Tavakoli, H.Z., Bahrami-Bavani, M., Miyanmahaleh, Y., Tajer-Mohammad-Ghazvini, P., 2021. Identification and characterization of a metal-resistant *Acidithiobacillus ferrooxidans* as important potential application for bioleaching. *Biologia (bratisl.)* 76, 1327–1337. <https://doi.org/10.1007/s11756-021-00687-z>.
- Wang, J., Cui, Y., Chu, H., Tian, B., Li, H., Zhang, M., Xin, B., 2022. Enhanced metal bioleaching mechanisms of extracellular polymeric substance for obsolete LiNi<sub>0.8</sub>Co<sub>0.1</sub>Mn<sub>0.1</sub>-x-yO<sub>2</sub> at high pulp density. *J. Environ. Manage.* 318, 115429. <https://doi.org/10.1016/j.jenvman.2022.115429>.
- Welcher, F.J., Hahn, R.B., 1964. Semi-micro qualitative analysis, in: *Encyclopedia of Chemical Technology*.
- Wu, W., Li, X., Zhang, X., Gu, T., Qiu, Y., Zhu, M., Tan, W., 2020. Characteristics of oxidative stress and antioxidant defenses by a mixed culture of acidophilic bacteria in response to Co<sup>2+</sup> exposure. *Extremophiles* 24, 485–499. <https://doi.org/10.1007/s00792-020-01170-4>.
- Xin, Y., Guo, X., Chen, S., Wang, J., Wu, F., Xin, B., 2016. Bioleaching of valuable metals Li, Co, Ni and Mn from spent electric vehicle Li-ion batteries for the purpose of recover. *J. Clean. Prod.* 116, 249–258. <https://doi.org/10.1016/j.jclepro.2016.01.001>.
- Zeng, X., Li, J., Singh, N., 2014. Recycling of spent lithium-ion battery: a critical review. *Crit. Rev. Environ. Sci. Technol.* 44, 1129–1165. <https://doi.org/10.1080/10643389.2013.763578>.
- Zhang, S., Yan, L., Xing, W., Chen, P., Zhang, Y., Wang, W., 2018. *Acidithiobacillus ferrooxidans* and its potential application. *Extremophiles* 22, 563–579. <https://doi.org/10.1007/s00792-018-1024-9>.
- Zhang, X., Shi, H., Tan, N., Zhu, M., Tan, W., Daramola, D., Gu, T., 2023. Advances in bioleaching of waste lithium batteries under metal ion stress. *Bioresour. Bioprocess.* 10. <https://doi.org/10.1186/s40643-023-00636-5>.
- Zhao, S., He, W., Li, G., 2019. Recycling Technology and Principle of Spent Lithium-Ion Battery, in: *Recycling of Spent Lithium-Ion Batteries*. Springer International Publishing, Cham, pp. 1–26. [https://doi.org/10.1007/978-3-030-31834-5\\_1](https://doi.org/10.1007/978-3-030-31834-5_1).
- Zimmermann, R., 1977. Estimation of Bacterial Number and Biomass by Epifluorescence Microscopy and Scanning Electron Microscopy. *Microbial Ecology of a Brackish Water Environment*. 103–120. [https://doi.org/10.1007/978-3-642-66791-6\\_10](https://doi.org/10.1007/978-3-642-66791-6_10).